Available online at www.sciencedirect.com
SCIENCE DIRECT®
ELSEVIER
Journal of Sound and Vibration 294 (2006) 916–926
JOURNAL OF SOUND AND VIBRATION
www.elsevier.com/locate/jsvi

Ridges reconstruction based on inverse wavelet transform

Jing Lin

National Laboratory of Acoustics, Institute of Acoustics, Chinese Academy of Sciences, P.O. Box 2712, Beijing 100080, PR China

Received 15 November 2004; received in revised form 19 April 2005; accepted 16 December 2005
Available online 28 February 2006

Abstract

Ridges always carry important physical information in practice. Ridge reconstruction based on inverse wavelet transform is studied in this article. It is emphasized that the points within the neighbor area have to be added in the reconstruction to avoid energy lost. However, no discussion has been proposed about how to choose the neighbor area up to now although it is the key to achieve good performance. A formula is given in this article to calculate the width of the neighbor area, which varies with scale and the signal itself. Some examples are given in this article to show the performance of the proposed method, which manifests that the method works very well for signals with multiple components as long as there is no cross section between them. It also works well when the signal to noise ratio is not very low.

1. Introduction

Generally speaking, ridge is the curve on the time-scale plane that is composed of local maxima with respect to scale. For frequency modulated (FM) signals, they always appear as ridges on the time-scale plane after wavelet transform. The ridge carries crucial information about the modulated components, such as instantaneous frequency and amplitude damping. A lot of discussions on wavelet ridge detection and reconstruction have been proposed in recent years [1,2] for this reason. For example, it has been successfully used to identify the damping parameters for multi-degree-of-freedom systems [3–5]. Various methods for ridge detection have been proposed [1,2], however, it is not the focus of this article. The method proposed in this article is on how to extract the component as complete as possible after the ridge has been detected already.

Ridge can be derived by some optimizing-based methods such as the penalization approach [2,6] for the purpose of data compression or noise resistance. However, for the method of penalization approach, the computation burden will increase dramatically as the data length goes up. It is not adapted to the case of signals associated with multiple ridges as well. As mentioned in Refs. [2,6], ridge reconstruction based on inverse wavelet transform or ‘‘skeleton reconstruction’’ can attain good accuracy and is very easy to be implemented. In the cases when the signal to noise ratio (SNR) is not very low, this method is a good choice. Unfortunately, up to now, ridge reconstruction based on inverse wavelet transform has not been investigated deeply. The discussion in this article is on how to get perfect ridge reconstruction by using inverse wavelet transform.

E-mail address: jing_lin00@sina.com.

0022-460X/$ - see front matter © 2006 Elsevier Ltd. All rights reserved.
doi:10.1016/j.jsv.2005.12.027

The energy of an instantaneous component will be spread on the time-scale plane due to window effect. Ridge is composed of local maxima instead of the points on total spread area. As a result, a lot of energy may be lost if only the points on the ridge are reconstructed. The wavelet coefficients in neighbor area must be added in the reconstruction in order to obtain good performance. The choice of the neighbor area affects the reconstruction accuracy significantly. Detail discussion is given in this article on how to choose a proper neighbor area for reconstruction. A general rule is proposed subsequently and a few examples are given to validate this rule. Ridge reconstruction given in this article also provides a new solution for multiple modes analysis in vibration and acoustic processing.

This paper is organized as follows. A brief review about wavelet transform and inverse wavelet transform is given in Section 2. The definition of the neighbor area is derived in Section 3. In Section 4, three examples are given to show the efficiency of the proposed method and some discussions are given as well. Finally, the conclusions are given in Section 5.

2. Review of wavelet transform and inverse wavelet transform

Let $\varphi(t)$ be the basic wavelet function, the daughter wavelet $\varphi_{a,b}(t)$ is given by the dilation and translation of $\varphi(t)$,

$$\varphi_{a,b} = \frac{1}{\sqrt{a}}\varphi\left(\frac{t-b}{a}\right). \tag{1}$$

The continuous wavelet transform of signal $x(t)$ is defined as

$$W_{a,b} = \int x(t)\overline{\varphi_{a,b}(t)}\,\mathrm{d}t = \frac{1}{\sqrt{a}}\int x(t)\overline{\varphi\left(\frac{t-b}{a}\right)}\,\mathrm{d}t, \tag{2}$$

where $\overline{\varphi_{a,b}(t)}$ is the complex conjugate of $\varphi_{a,b}(t)$.

The basic wavelet $\varphi(t)$ should meet the admission condition

$$C_\varphi = \int_{-\infty}^{\infty} \frac{|\hat{\varphi}(\omega)|^2}{|\omega|}\,\mathrm{d}\omega < \infty, \tag{3}$$

where $\hat{\varphi}(\omega)$ is the Fourier transform of $\varphi(t)$.

For a real signal $x(t)$, there is a standard wavelet inversion formula as follows:

$$x(t) = \frac{2}{C_\varphi}\mathrm{Re}\int_0^{\infty}\frac{\mathrm{d}a}{a^2}\int_{-\infty}^{\infty}\mathrm{d}b\,W_{a,b}\varphi_{a,b}, \tag{4}$$

where Re indicates the real part and C_φ is given by Eq. (3).

Usually, the single integral formula is employed for simplicity [7]

$$x(b) = \mathrm{Re}\frac{2}{C_{1\varphi}}\int_0^{\infty}\frac{\mathrm{d}a}{a^{3/2}}W_{a,b}, \tag{5}$$

where

$$C_{1\varphi} = \int_{-\infty}^{\infty}\frac{\hat{\varphi}(\omega)}{|\omega|}\,\mathrm{d}\omega. \tag{6}$$

Inverse wavelet transform provides a solution for feature extraction or noise removal for signals. If all the wavelet coefficients corresponding to the feature component are known, the feature component can be obtained by only reconstructing those coefficients via Eq. (5).

3. Ridge reconstruction via inverse wavelet transform

In applications, feature components are always required to be extracted as complete as possible. Incomplete recover of the feature components may cause improper evaluation of the system being studied. As stated in

Refs. [2,6], the method of "skeleton reconstruction" is considered as a naive, however, almost errorless reconstruction. Compared with the current methods, such as penalization approach, it is much easier to be implemented and has much less computation especially when data length is very big. Up to now, the "skeleton reconstruction" method almost remains unexploited, except that the feasibility and the performance of the method were pointed out. No report was given clearly that if we need to add the points within the neighbor area of the ridge and how wide the neighbor should be. In this section, the "skeleton reconstruction" method is studied. Firstly, some examples are given to show that a lot of energy may be lost if only the points on the ridge are reconstructed. Secondly, a general rule is given on how to define the neighbor area of the ridge for reconstruction.

3.1. Illustrations

A simulation is given as follows to show how bad the performance is when the points only on the ridge are reconstructed. The simulated signal is given in Fig. 1. It is a frequency modulated signal with fast amplitude decaying.

Morlet wavelet is used to take the wavelet transform throughout the article. The definition of Morlet wavelet is

$$\psi(t) = \mathrm{e}^{-\frac{\beta^2 t^2}{2}} \mathrm{e}^{-\mathrm{j}\omega t}. \tag{7}$$

Only the real part of the function is used as the basic wavelet. Fig. 2 gives the continuous wavelet transforms of the signal.

Take some points on the ridge (any current methods can be used here to find the local maxima) and use the cubic spline function to interpolate those points, we can get a smooth curve to approximate the ridge, as shown in Fig. 3.

The reconstruction result is given in Fig. 4. The original signal is also shown in the same picture for comparison. It can be easily found that most energy is lost after reconstruction.

The reason can be summarized as follows. Wavelet function is localized both in time domain and frequency domain. Wavelet transform is to view the signal via the windows with different dilations. At each scale the instantaneous energy of the signal at time t is dispersed on the neighbor area of t. The width of the neighbor area depends on wavelet function and the signal itself, which will be discussed in the following part.

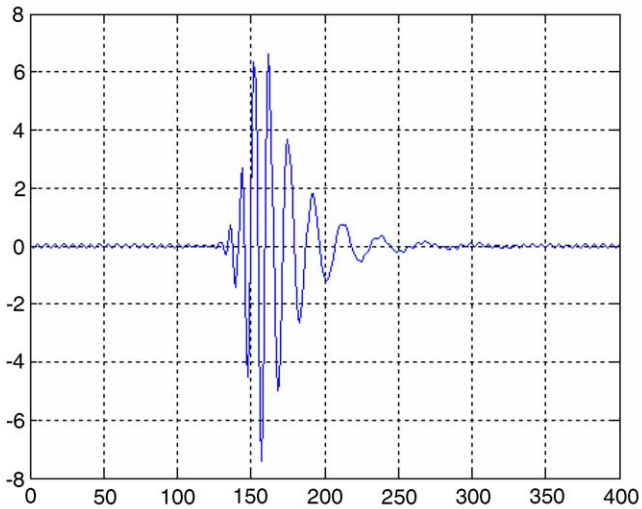

Fig. 1. The waveform of the simulated signal.

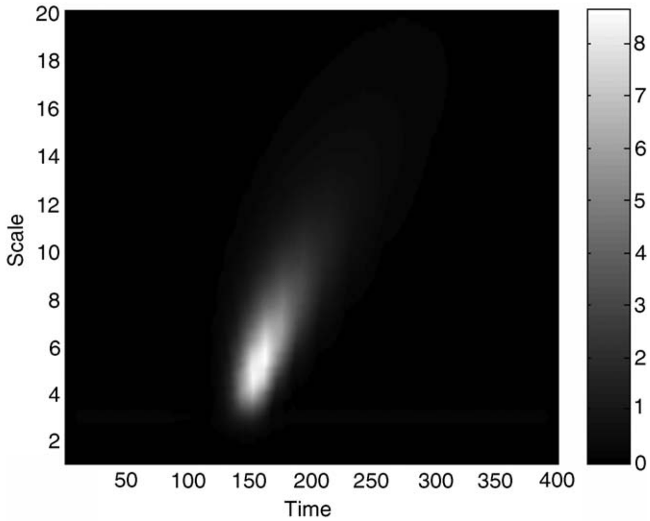

Fig. 2. Continuous wavelet transform of the simulated signal.

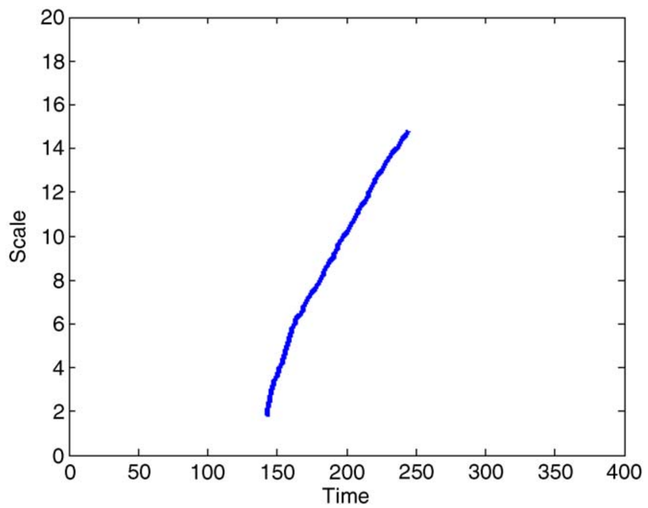

Fig. 3. Ridge of the signal on time-scale plane.

3.2. *Choice of the neighbor area*

The width of the neighbor has to be chosen properly. Too much noise will be incorporated in the reconstruction if the neighbor area is taken too big, too much energy will be lost if the neighbor area is taken too small. For a frequency modulated signal, the energy of the signal can be imaged distributed within a tube after wavelet transform, as shown in Fig. 5. The central axis of the tube is the ridge of the signal.

The shadow area in Fig. 5 is the frequency band with respect to scale a. Δt_2 is the time duration of the signal at scale a. Δt_1 is the time taken by the signal varying form instantaneous frequency f_2 to f_1. The rest part of the time duration $\Delta t_2 - \Delta t_1$ is caused by the window effect of the son wavelet with respect to scale a.

It is relatively difficult to define the time duration Δt_1, because it is totally up to the signal itself and usually we have no prior knowledge about what it is. Actually, the time duration Δt_1 can be obtained by using the slope of the ridge on the time-scale plane at each point. The function of the ridge can be

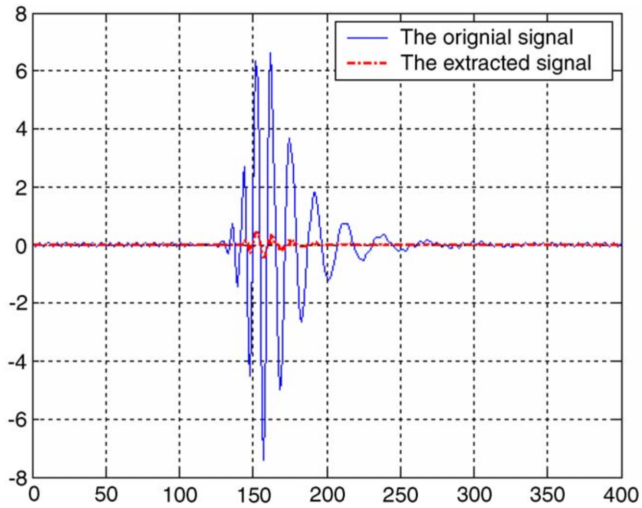

Fig. 4. Reconstruction of the ridge.

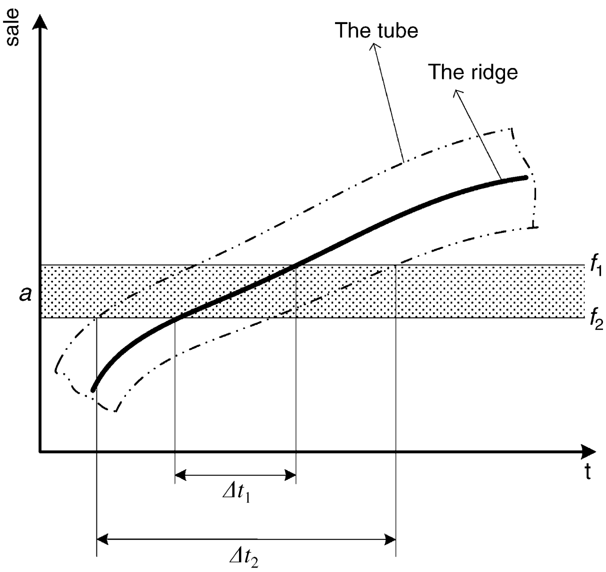

Fig. 5. Illustration of ridge and its neighbor area on time-scale plane.

approximated by polynomial interpolation, and the slope at each point can be obtained via derivation. Therefore, there exists

$$\Delta t_1 = \frac{\Delta a}{|k|}, \tag{8}$$

where k is the slope of the curve at scale a.

As we know, Morlet wavelet does not satisfy the admission condition strictly. Accordingly, the energy of the signal would spread on all the wavelet coefficients due to convolution, however, with different contribution on different coefficients. In the case when the signal has no noise and only has one ridge, the errorless reconstruction is to reconstruct all the wavelet coefficients. Of course it is meaningless for practical cases. Generally, the optimal width of the integration window is up to the SNR, the probability density function of the noise, the rule for risk evaluation and the signal itself. The signal content is decreasing as the integration window goes big, however, the noise content is increasing as well at the same time. So there always exists an optimal width of the window to make it have minimal reconstruction error.

For the son wavelet $\varphi_a = \mathrm{e}^{-\beta^2 t^2/2a^2}\mathrm{e}^{-j\omega t}$, the standard deviation is

$$\sigma_t = \frac{\Delta a}{\sqrt{2}\beta}. \tag{9}$$

Suppose the width of the son wavelet window is taken $[t_0 - M\sigma_t, t_0 + M\sigma_t]$, $M \geqslant 0$, we can get the width of the integration window at scale a by combining Eqs. (8) and (9),

$$\Delta t_2 = \frac{\sqrt{2}Ma}{\beta} + \frac{\Delta a}{|k|}. \tag{10}$$

Suppose the sampling rate is S_f, the number of the points within the neighbor area associated to scale a is

$$N = \frac{\Delta a}{|k|}S_f + \frac{\sqrt{2}Ma}{\beta}S_f. \tag{11}$$

According to the theory of statistics, over 90% of the total energy inside the window is centered in the area of $[t_0 - 2\sigma_t, t_0 + 2\sigma_t]$, where t_0 is the time location of the ridge with respect to scale a. At the same time, Gaussian window (the envelop of the wavelet) is decaying very slowly when beyond $2\sigma_t$, the window width of the son wavelet with respect to scale a can be taken $4\sigma_t$ for general case, i.e., the noise is not too heavy and the distance between any two adjacent components is bigger than the sum of the half width of the two components at each scale. In this case, M takes 2 in Eqs. (10) and (11).

4. Applications and discussions

In this section, some signals are used to validate the proposed method. Discussions are given based on the results.

4.1. Examples

Three examples are given in this section to show the efficiency of the proposed method. The signal shown in Fig. 1 is taken as the first example here. Fig. 6 gives the comparison between the reconstruction result and the original signal. It can be easily found that the reconstruction is almost errorless.

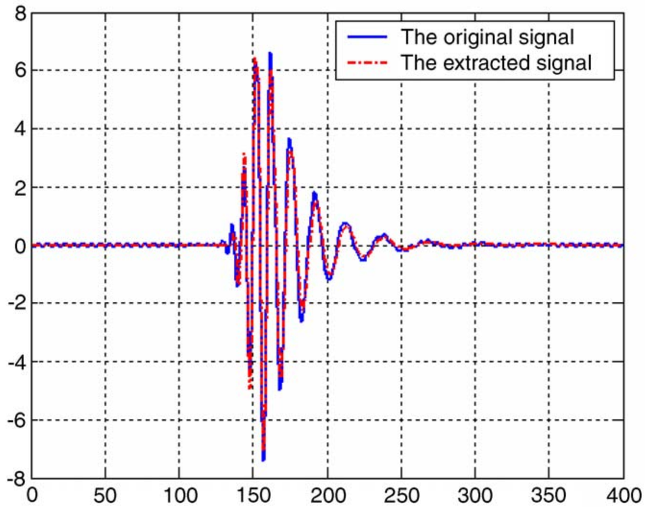

Fig. 6. Reconstruction of the ridge and its neighbor area.

In some cases, there are several ridges in a signal. Therefore, the reconstruction method has to be applicable to signals with multiple FM components. The second example given as follows is to show the performance of the proposed method for this case. Fig. 7 is the waveform of the signal with four FM components. Fig. 8 is the continuous wavelet transform of the signal. The four ridges can be observed clearly from the picture.

By using the proposed method to extract the four FM components one by one, we get the results shown in Fig. 9. The waveform of each FM component is also given in Fig. 9 for comparison. The reconstruction error of component #1, #2, #3 and #4 are, respectively, 2.2%, 2.1%, 2.1% and 2.8%.

In practice, it is always inevitable to introduce noise in signals. As a result, the method should be robust to noise to some extent. Another example given as follows is to show the performance for noise resistance. Fig. 10 is the waveform of the noisy signal composed of the signal shown in Fig. 7 and Gaussian noise with zero mean and variance 2. The SNR is 0 dB. For simplicity, only component #2 is extracted and the result is

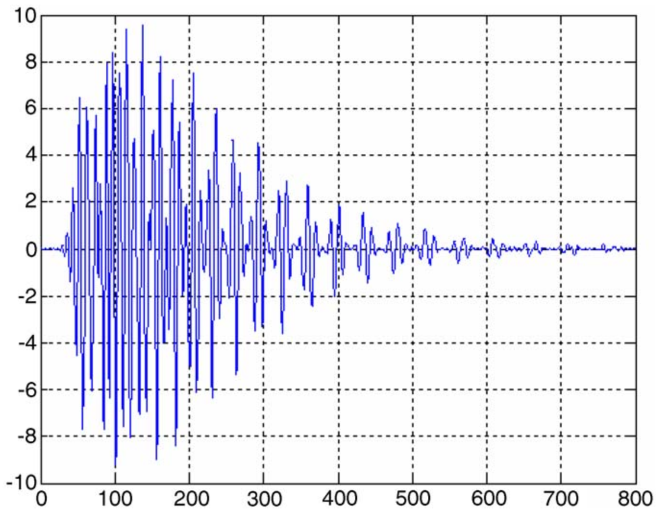

Fig. 7. Waveform of the signal with multiple components.

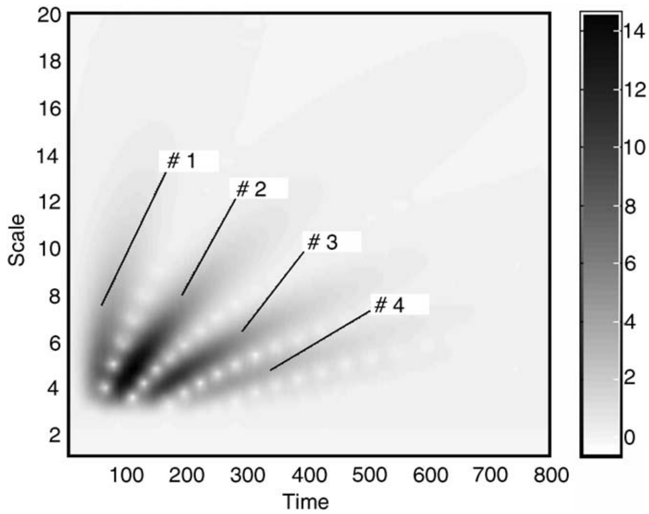

Fig. 8. Continuous wavelet transform of the signal with multiple components.

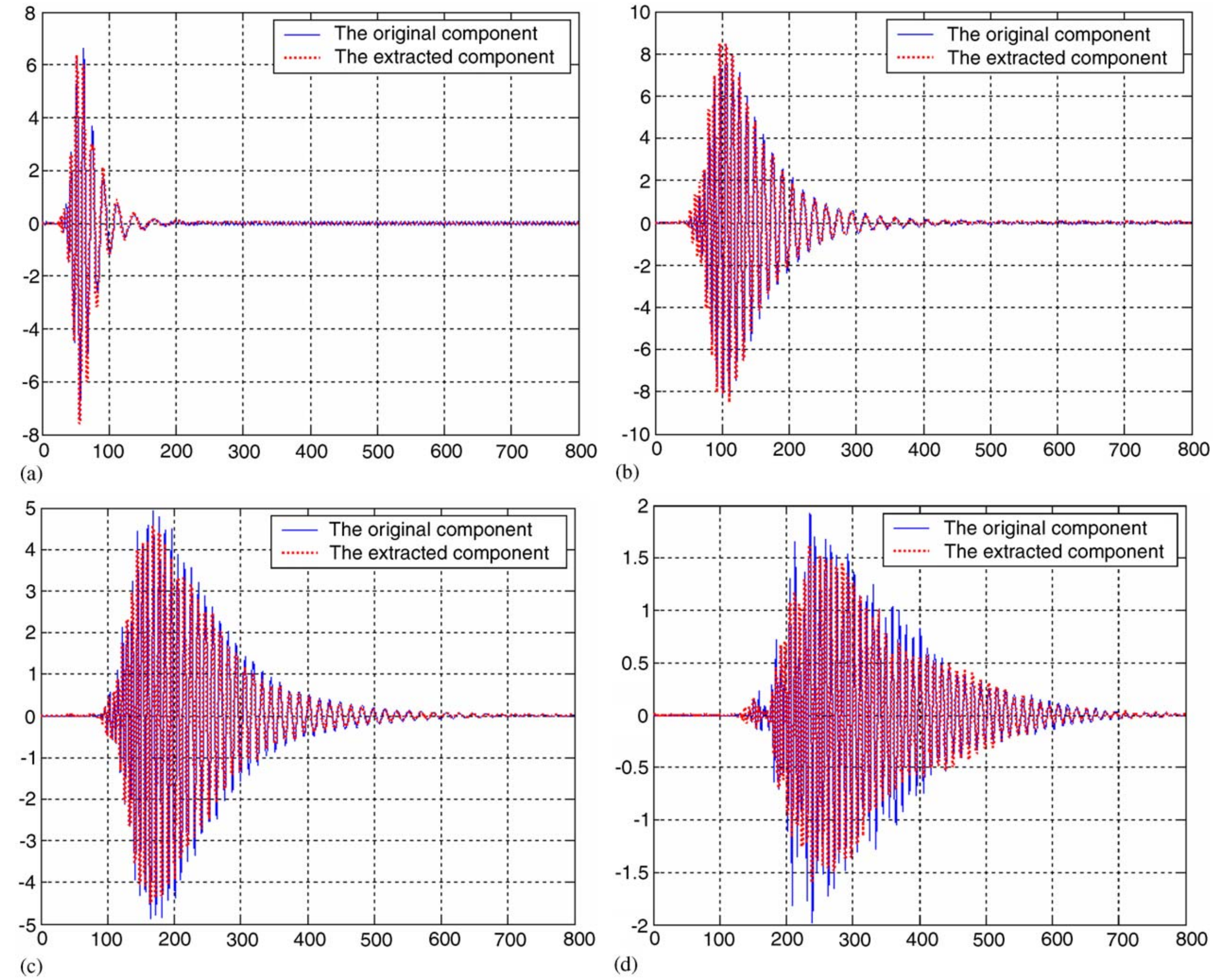

Fig. 9. (a) Reconstruction result of component #1 with 2.2% error. (b) Reconstruction of component #2 with 2.1% error. (c) Reconstruction result of component #3 with 2.1% error. (d) Reconstruction result of component #4 with 2.8% error.

given in Fig. 11. The original component is also given in Fig. 11 for comparison. The SNR of the reconstruction result is 12 dB.

4.2. Discussions

From the illustration shown in Figs. 6, 9 and 11 we can find that the reconstruction is perfect when no noise is contained. However, different FM components must have no cross section. At the same time, the proposed method is also resistance to noise to some extent. Actually, the SNR of the reconstruction can be further improved by thresholding technique [8], i.e., using some certain threshold to process the wavelet coefficient to eliminate the effect of noise before reconstruction.

As stated in Section 3, the width of the integration window also depends on SNR and the signal itself. In the following, a simulation is done to show how the reconstruction error varies with the width of the integration window and how the performance varies with the introduction of noise. In the test, width parameter M in Eq. (10) varies from 0 to 3, and Gaussian noise is also added to show how it affects the width of the window. The relationship between reconstruction error and M value of the four FM components is given in Fig. 12. The waveforms of the four FM components have been shown in Fig. 7. It can be seen in Figs. 8 and 9 that the

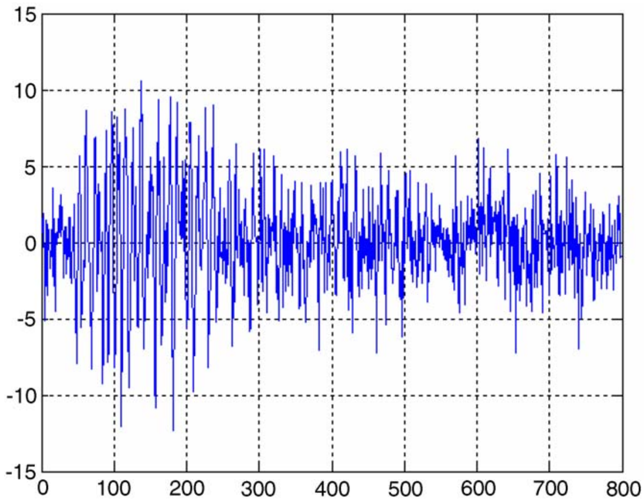

Fig. 10. The noisy signal (SNR = 0 dB).

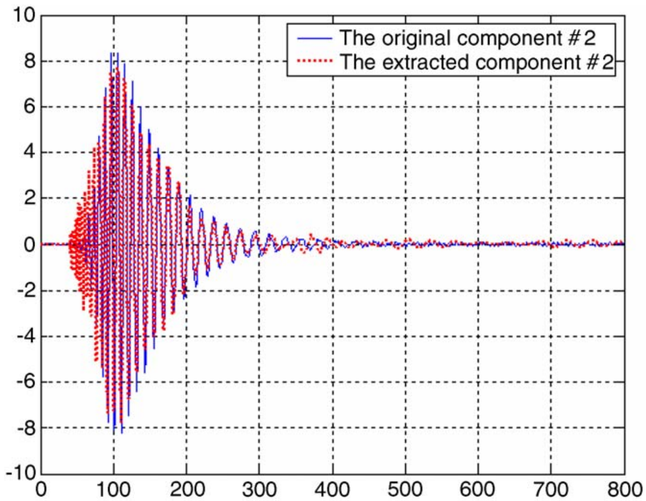

Fig 11. The reconstruction of the component #2 (SNR = 12 dB).

four components have different frequency range and damping rate. Let D_j represent the damping rate of the jth component, B_j represent the frequency range of the jth component. There exist $D_1 > D_2 > D_3 > D_4$ and $B_1 > B_2 > B_3 > B_4$. It can be seen in Fig. 12 that the reconstruction error is decreasing significantly as M increases from 0 to 1.5 for all components. When M goes beyond 1.5, the reconstruction error decreases slowly except component #1. The reconstruction error for component #1 is increasing when M varies from 1.5 to 3. The reason lies that the contribution from other components increases faster than that from component #1 when M goes from 1.5 to 3. The result in Fig. 12 shows that when the width of the integration window is big enough, the reconstruction error will decrease slowly when the width goes on increasing.

The following picture gives the relationship between reconstruction error and M when noise is contained, as shown in Fig. 13. The waveform of the noisy signal is shown in Fig. 10. The result is very different with that given in Fig. 12.

The variations can be summarized as follows:

(i) The values of M with respect to the minimal reconstruction error become small.
(ii) The reconstruction error with respect to the same value of M becomes big.

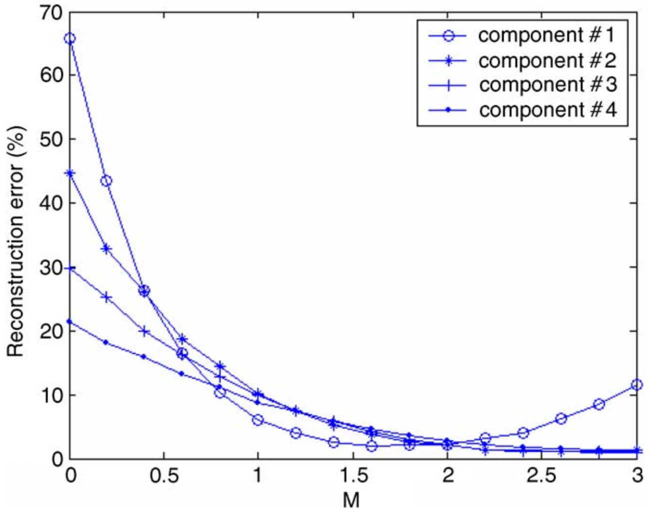

Fig 12. Reconstruction error versus M when signal has no noise.

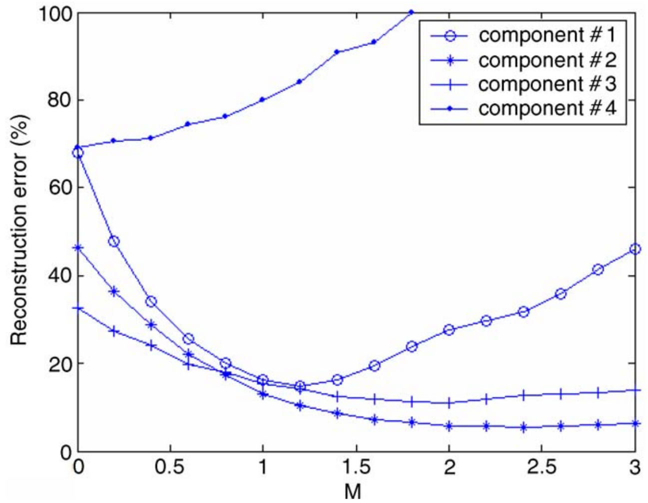

Fig 13. Reconstruction error versus M when signal contains noise.

(iii) The curve with respect to component #4 is very different with others. The reconstruction error is increasing monotonously as M goes big. The error even exceeds 100% when M is over than 1.8.

The reason can be explained as follows:

(i) Noise content is increasing as the window goes big.
(ii) The SNR in each integration window becomes small because of noise.
(iii) For component #4, it is almost a flatten curve on time-scale plane, as shown in Fig. 8. According formula (10), the width of the integration window is also up to the slope of the curve. The width can be very big when the slope takes a small value. More noise will be contained in this case.

In a word, the reconstruction error can keep a relative low level when M takes 2 for noise free signal. The value will be less when signal contain noise.

5. Conclusions

In wavelet analysis, ridges can be reconstructed via inverse wavelet transform. In the reconstruction, not only the points on the ridge but also those within the neighbor area of the ridge need to be reconstructed in order to get good performance. A proper definition of the neighbor area is the key to achieve an accurate reconstruction. A formula is given on how to choose the neighbor area for ridge reconstruction. Some examples are given to show good performance of the method. Some conclusions can be drawn from the simulation as follows:

(i) For the signal without noise, the reconstruction error is small enough when M takes 2 in formula (10) whenever what kind of signal it is.
(ii) For the signal with sharp variation of frequency (such as component #1), the integration window is smaller than that of the signal with slow variation of frequency (such as component #2).
(iii) For the signal with noise, the optimal width of the integration window is smaller than that of the same signal without noise.
(iv) For signal with neither sharp nor slow variation (such as components #2 and #3), the window width defined in this paper is robust to noise, for example, the SNR can be improved from 0 to 12 dB for component #2.

References

[1] N. Delprat, et al., Asymptotic wavelet and gabor analysis: extraction of instantaneous frequencies, *IEEE Transactions on Information Theory* 38 (1992) 644–664.
[2] R. Carmona, W.L. Hwang, B. Torrésani, Characterization of signals by the ridges of their wavelet transforms, *IEEE Transactions on Signal Processing* 45 (1997) 2586–2590.
[3] J. Slavic, I. Simonovski, M. Boltezar, Damping identification using continuous wavelet transform: application to real data, *Journal of Sound and Vibration* 262 (2003) 291–307.
[4] W.J. Staszewski, Identification of non-linear systems using multi-scale ridges and skeletons of the wavelet transform, *Journal of Sound and Vibration* 214 (1998) 639–658.
[5] J. Lardies, S. Gouttebroze, Identification of modal parameters using the wavelet transform, *International Journal of Mechanical Sciences* 44 (2002) 2263–2283.
[6] R. Carmona, W.L. Hwang, B. Torrésani, Multiridge detection and time-frequency reconstruction, *IEEE Transactions on Signal Processing* 47 (1999) 480–492.
[7] M.J. Shensa, Discrete inverses for nonorthogonal wavelet transform, *IEEE Transactions on Signal Processing* 44 (1996) 798–807.
[8] D.L. Donoho, Denoising by soft-thresholding, *IEEE Transactions on Information Theory* 41 (1995) 613–627.